ELSEVIER

Physica A 282 (2000) 283–303

PHYSICA A

www.elsevier.com/locate/physa

Reaction–diffusion modelling of bacterial colony patterns

Masayasu Mimura[a,*], Hideo Sakaguchi[b], Mitsugu Matsushita[c]

[a] *Institute for Nonlinear Sciences and Applied Mathematics, Graduate School of Science, Hiroshima University, Higashi-Hirosima 739-8526, Japan*

[b] *Department of Mathematics, Faculty of Engineering, Tokushima University, Tokushima 770-8506, Japan*

[c] *Department of Physics, Chuo University, Tokyo 112-8551, Japan*

Received 27 September 1999; received in revised form 26 January 2000

Abstract

It is well known from experiments that bacterial species *Bacillus subtilis* exhibit various colony patterns. These are essentially classified into five types in the morphological diagram, depending on the substrate softness and nutrient concentration. (A) diffusion-limited aggregation-like; (B) Eden-like; (C) concentric ring-like; (D) disk-like; and (E) dense branching morphology-like. There arises the naive question of whether the diversity of colony patterns observed in experiments is caused by different effects or governed by the same underlying principles. Our research has led us to propose reaction–diffusion models to describe the morphological diversity of colony patterns except for Eden-like ones.

Keywords: Pattern formation; Bacterial colony; Reaction–diffusion models

1. Introduction

It is known from experiments that colonies of bacterial species called *Bacillus subtilis* exhibit diverse growth patterns on the surface of thin agar plates by feeding on the nutrient. Such colony patterns drastically change when only two environmental conditions, the concentrations of agar and nutrient, say C_a, and C_n are varied [1,2]. As in Fig. 1.1, these are qualitatively classified into five types of patterns, each of which is observed in the regions labeled as A–E in the (C_n, C_a^{-1})-plane [3]. If C_n is low and C_a is high, as in the region A (hard agar medium with poor nutrients),

* Corresponding author.

E-mail address: mimura@math.sci.hiroshima-u.ac.jp (M. Mimura)

0378-4371/00/$ - see front matter
PII: S0378-4371(00)00085-6

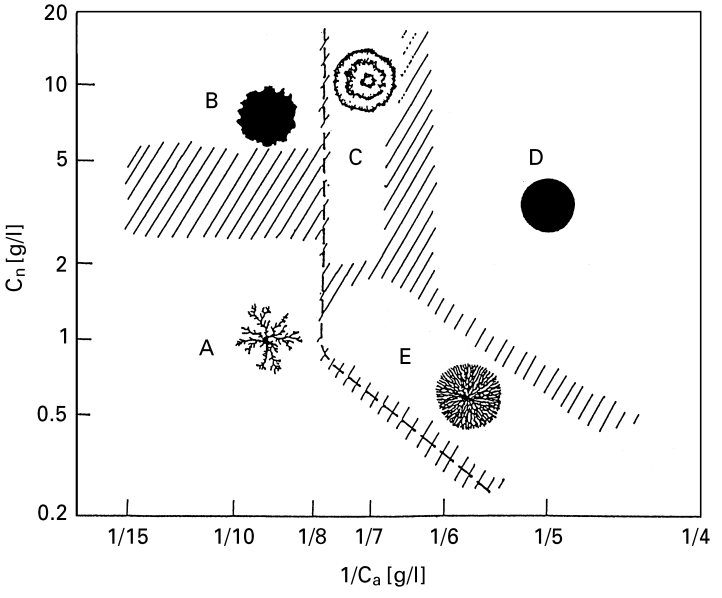

Fig. 1.1. Morphological diagram of *B. subtilis* colony patterns.

the colony pattern shows dendritic growth with characteristically branched structures, which are quite similar to those of diffusion limited processes in solidification from a super-saturated solution, solidification from undercooled liquid and electro-chemical depositions. Also, these are clearly reminiscent of two-dimensional diffusion-limited aggregation (DLA) clusters [4], which can be generated by a simple particle model for randomly branching patterns grown through diffusion-limited processes [5]. If C_n is increased with fixed C_a being high, each branch becomes thicker and thicker and then the colony has a roughly round shape with rough envelope, as in the region B (see, e.g., Ref. [6]) [7]. On the contrary, if C_a is decreased with fixed C_n being low, as in the region E [8], the colony shows a pattern similar to the so-called dense-branching morphology (DBM) where the advancing envelope looks characteristically smooth. In the region D [3] where C_n is high and C_a is low (soft agar medium with rich nutrients), the colony is homogeneously spreading, and develops macroscopically a disk-like pattern where the movement of bacteria can be described in terms of diffusion. Finally, in the region C, bacteria actively move and suddenly stop while performing cell-division, and repeating this cycle, the resulting colony exhibit concentric ring pattern.

The above observations give the following naive question:

Is the diversity of such colony patterns caused by different effects or governed by the same underlying principles?

In order to answer this question from a theoretical standing point, various types of continuous and discrete models have been already proposed [3,9–14]. Among them, there are reaction–diffusion (RD) models in which the spatial and temporal change of bacteria are described by using their averaged densities.

Letting $b(t,x)$ be the population density of bacteria at time t and position x, we begin with introducing the following RD model which is called the Fisher equation:

$$b_t = d\Delta b + (\varepsilon - \mu b)b\,, \tag{1.1}$$

where d is the diffusion rate of bacteria, ε is the given concentration of nutrients and μ is the intra-specific competition rate among bacterial cells. All of them are positive constants. If $b(0,x) = b_0(x)$ takes one point-like distribution on the plane, then the solution $b(t,x)$ homogeneously spreads like an expanding disk. Wakita et al. [3] confirmed that it is well consistent with the experimentally observed pattern in the region D.

As was noted above, growth patterns of colonies drastically depend on the initial concentration of nutrients. Therefore, it is plausible to introduce the concentration of nutrients, say $n(t,x)$ as another unknown variable. Consequently, (1.1) is altered as follows:

$$\begin{aligned} b_t &= d\Delta b + vg(n)b\,, \\ n_t &= \Delta n - g(n)b\,, \end{aligned} \tag{1.2}$$

where $g(n)$ is the growth rate of bacteria. A widely used form of $g(n)$ is the Michaelis–Menten kinetics

$$g(n) = \frac{\alpha n}{1+\beta n}$$

with positive constants α and β [15], where v is the conversion rate of nutrients into growth but we may put $v = 1$ without loss of generality. We take the initial conditions to (1.2) as

$$\begin{aligned} b(0,x) &= b_0(x)\,, \\ n(0,x) &= n_0\,, \end{aligned} \tag{1.3}$$

where n_0 is a positive constant, because the initial concentration of nutrients is constantly distributed in experiments. We may think that two parameters d and n_0 respectively correspond to C_a^{-1} and C_n in the experiments. Taking $d = 1$, for instance, one obviously knows that (1.2) and (1.3) lead to

$$\begin{aligned} (b+n)_t &= \Delta(b+n)\,, \\ (b+n)(0,x) &= b_0(x) + n_0\,. \end{aligned} \tag{1.4}$$

If $b_0(x)$ is very small, that is, $b_0(x)+n_0 \approx n_0$, then one knows that $b(t,x)+n(t,x) \equiv n_0$ approximately holds so that the first equation of (1.2) can be written as

$$b_t = d\Delta b + g(n_0 - b)b\,. \tag{1.5}$$

If $g(n)$ takes the simplest form $g(n) = \alpha n$ (Malthusian growth), (1.5) is essentially the same as (1.1). In this sense, (1.2) is very close to (1.1). Numerical calculation of (1.2) with (1.3) shows that $b(x,t)$ homogeneously spreads for any values of d and n_0, where

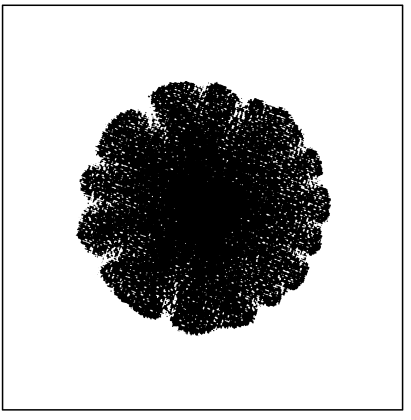

Fig. 1.2. Front instability of a disk-like pattern in Kessler and Levine model (1.6) where $d = 0.01$, $g(n) = n$, $\theta = 0.25$.

the spreading velocity is asymptotically given by $2\sqrt{dn_0}$. It turns out that the growth of bacteria is limited by nutrient concentration and bacterial diffusion. When d and n_0 are large, the system (1.2) is a good description of disk-like patterns in the region D. However, we should note that, even if d and n_0 are small, (1.5) or (1.2) with (1.3) does not reproduce any branched patterns observed in the regions A–C and E.

For the occurrence of branched patterns in the framework of (1.2), Kessler and Levine [16] include a cutoff mechanism into the growth term $g(n)$ in (1.2). The resulting system is

$$b_t = d\Delta b + H(b-\theta)g(n)b\,,$$
$$n_t = \Delta n - H(b-\theta)g(n)b\,, \tag{1.6}$$

where $H(b-\theta)$ is the heaviside function with some threshold density $\theta > 0$. This alteration possibly causes front instability, as in Fig. 1.2, but it does not seem to generate branched patterns. In order to produce such patterns, Golding et al. [9] add a death term $-\mu b$ with constant $\mu > 0$ to (1.6) and offer the following model:

$$b_t = d\Delta b + H(b-\theta)g(n)b - \mu b\,,$$
$$n_t = \Delta n - H(b-\theta)g(n)b\,. \tag{1.7}$$

Although this term enables to produce branched patterns, as in Fig. 1.3, these do not seem to resemble clearly branched patterns observed in experiments.

Kawasaki et al. [11] remarked that bacteria can hardly move when either the concentration of nutrients or the density of bacteria are lower, and assumed that the diffusion coefficient of bacteria is not constant but depends on their own density as well as the concentration of nutrients. They proposed the following nonlinear diffusion model:

$$b_t = d\nabla((1+\omega(x))nb\nabla b) + nb\,,$$
$$n_t = \Delta n - nb\,, \tag{1.8}$$

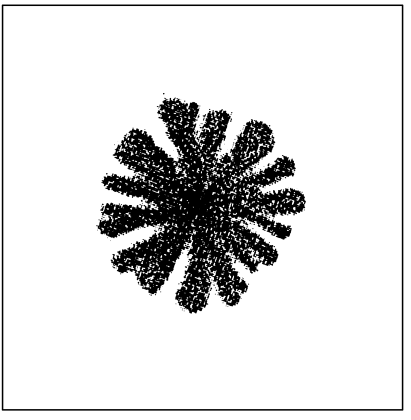

Fig. 1.3. Front instability of a disk-like pattern in (1.7) where d, $g(n)$ and θ are the same as in Fig. 1.2 except $\mu = 0.01$.

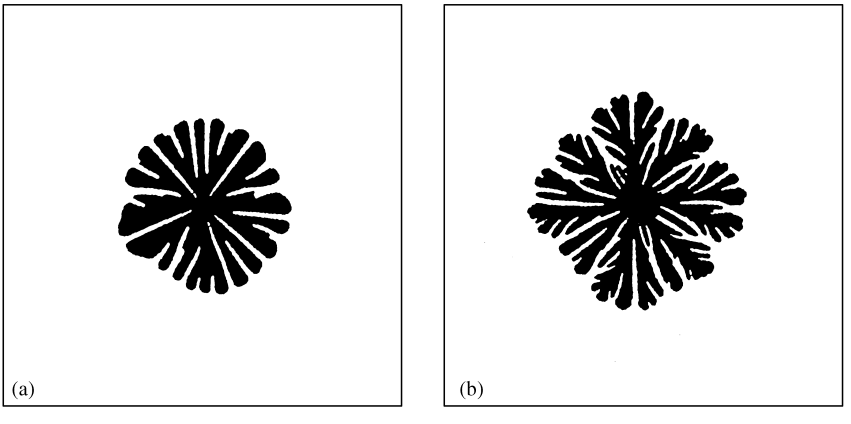

Fig. 1.4. Front instability of a disk-like pattern in Kawasaki et al. model (1.8) where $d = 1.0$, $v_0 = 0.71$, (a) $\omega(x) \equiv 0$, (b) $|\omega(x)| < 1.0$.

where $\omega(x)$ implies stochastic fluctuations of random movement of bacteria. This kind of nonlinear diffusion, which is degenerate at either $n = 0$ or $b = 0$, also causes front instability when $\omega(x) \equiv 0$, as in Fig. 1.4(a). When some fluctuations are included in the model, it is surprising that (1.8) reproduces branched patterns in experiments, as in Fig. 1.4(b). By this result, they emphasize that suitable fluctuations should be needed for the appearance of branched patterns.

Along the same line as (1.5)–(1.8), Kitsunezaki [12] proposes the following density-dependent diffusion model:

$$\begin{aligned} b_t &= d\nabla(b\nabla b) + nb - \mu b\,, \\ n_t &= \Delta n - nb\,, \\ s_t &= \mu b\,. \end{aligned} \tag{1.9}$$

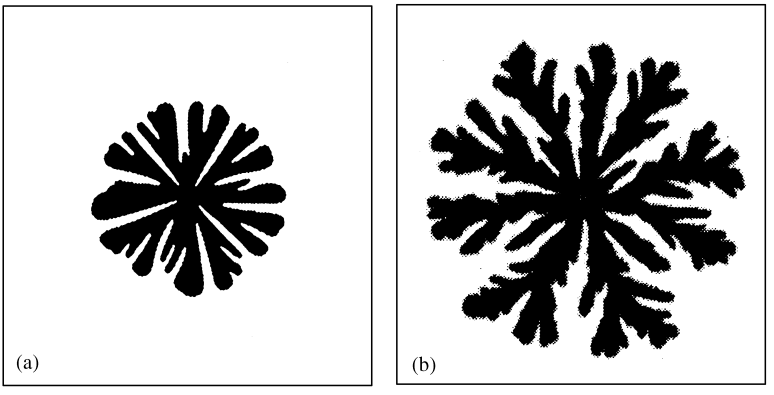

Fig. 1.5. Front instability of a disk-like pattern of $b + s$ in Kitsunezaki model (1.9) where $d = 0.10$, $\mu = 0.15$, $v_0 = 1.0$. (a) The averaged size of meshes h is about 0.5, (b) $h = 1.0$

The feature of this system is that the state of bacteria is separated into active and inactive states, where the active bacteria convert the inactive ones at some constant rate. In this model, b and s represent, respectively, the population densities of active and inactive bacteria and μ is the constant conversion rate. When d is suitably small, (1.9) also causes front instability but less tip-splitting, as in Fig. 1.5(a), and the resulting branched pattern seems to be slightly different from the experimentally observed one. However, if the system is discretized on rough and random mesh points, it well reproduces branched pattern in the region A, as in Fig. 1.5(b). The results indicate that rough and random discretization are importrant for (1.9) to generate branched patterns.

From more biological standing point, Golding et al. [9] have recently argued the effect of the lubricating field on the motion of bacteria, and introduced this effect into (1.9) to reproduce branched patterns.

Integrating the aboves, we have found that RD modelling gives a good description of colony patterns including not only spreading disk-like patterns but also branched ones, and both nonlinear diffusion models (1.8) and (1.9) possess the mechanism of front instability. Indeed, it is stated in [9] that nonlinear diffusion can be used to describe the movement of bacteria. Nevertheless, we should remark that these models by themselves do not reproduce branched patterns observed in experiments. The former needs to introduce suitable fluctuations in the diffusion coefficient, and the latter has to be discretized by relatively rough meshes.

Independent of the above models, the authors proposed the following RD model [17]:

$$u_t = \nabla(d(b)\nabla u) + uv - a(u,v)u\,,$$

$$v_t = \Delta v - uv, \quad t > 0,\ x \in \Omega\,,$$

$$w_t = a(u,v)u\,, \tag{1.10}$$

where u and w are, respectively, the population densities of the active and inactvie bacteria, and v is the concentration of nutrients. $d(b)$ is a function of the total density of bacteria $b = u + w$. $a(u,v)$ is the conversion rate from the active cells to the inactive ones. Eq. (1.10) is similar to (1.8) and (1.9), but there are the features that (i) active cells convert inactive ones with the rate $a(u,v)$ which depends on the density of active bacteria as well as the concentration of nutrients v; (ii) under the situation where the agar is semi-solid(soft) $d(b) = d_0$, which is constant, that is, it is normal diffusion; (iii) under the situation where the agar is solid(hard), $d(b) = d_1 b$ with constant $d_1 > 0$, nonlinear diffusion, which is different from the ones in (1.8) and (1.9), is introduced.

The aim of this paper is to study what kind of patterns (1.10) can generate, when two parameters corresponding to (C_a^{-1}, C_n) are varied.

In Section 2, we explain the derivation of (1.10), and in Sections 3 and 4, we consider the one-dimensional and two-dimensional growth patterns arising in (1.10), respectively. Finally, in Section 5, we give some remarks on our model.

2. An RD model

Motivated by the experimental observation [18], we assume that bacteria consist of two types; one is the active bacteria which move, grow and perform cell-division, while the other is the inactive ones which do nothing at all. Let $A(t,x)$ and $I(t,x)$ be, respectively, the densities of the active and inactive bacteria (the total density of the bacteria is given by $A(t,x) + I(t,x)$) and $N(t,x)$ be the concentration of nutrients at time t and position x. The model for A, I and N is

$$
\begin{aligned}
A_t &= \nabla(d_A \nabla A) + vg(N)A - a(A,N,I)A + b(A,N,I)I\,, \\
N_t &= d_N \Delta N - g(N)A\,, \\
I_t &= a(A,N,I)A - b(A,N,I)I\,,
\end{aligned} \tag{2.1}
$$

where d_A is the motility of the active bacteria and d_N is the diffusion rate of nutrients. $vg(N)$ is the growth rate with a positive constant v, $a(A,N,I)$ and $b(A,N,I)$ are the conversion rates between the active bacteria and the inactive ones.

First, we specify functional forms of d_A, d_N, $g(N)$, $a(A,N,I)$ and $b(A,N,I)$ in the model (2.1).

(i) *Motility of active bacteria*: d_A. The motility of bacteria is not so simple at a microscopic level. However, when the agar is soft (C_a is small), it may be presumably described by normal diffusion. On the other hand, when the agar becomes stiff (C_a is large), they hardly move but performing cell-division, the colony can expand by a sort of "population pressure" of bacteria [19]. Applying the idea of population pressure of biological individuals [19] to this situation, we propose a nonlinear diffusion $d_A = d_A(B)$ with the total density of bacteria $B = A + I$, which is monotonously increasing with B

satisfying $d_A(0)=0$. As a simple form of d_A, we take

$$d_A(B)=\begin{cases} d_0 & \text{for soft agar}\,, \\ d_1 B & \text{for hard agar}\,, \end{cases} \tag{2.2}$$

where d_0 and d_1 are suitable positive constants, which are decreasing the concentration of agar with C_a.

(ii) *Diffusion rate of nutrients*: d_N. Since nutrients diffuse in the agar, we take d_N to be a positive constant, which may weakly depend on C_a.

(iii) *Growth rate*: $g(N)$. It is plausible that the growth rate $g(N)$ is monotonically increasing with N. A typical form would be the Michaelis–Menten kinetics $g(N)=\alpha N/(1+\beta N)$ with positive constants α and β. For simplicity only, we take $\beta=0$ and specify $g(N)=\alpha N$ as the Malthusian growth rate.

(iv) *Active–inactive conversion rates*: $a(A,N,I)$ and $b(A,N,I)$. An important and essential core in our modeling is to specify the forms of $a(A,N,I)$ and $b(A,N,I)$. By the observation that once active bacteria become inactive ones, they never become active again unless food is added artificially, we neglect the conversion of the inactive cells into the active ones, that is, $b(A,N,I)\equiv 0$. Furthermore, we simply assume that $a(A,N,I)$ is independent of I. This simplification reduces system (2.1) to the following two-component system for A and N only:

$$\begin{aligned} A_t &= \nabla(d_A\nabla A)+\alpha vNA-a(A,N)A\,, \\ N_t &= d_N\Delta N-\alpha NA \end{aligned} \tag{2.3}$$

and I can be obtained through

$$I_t = a(A,N)A\,. \tag{2.4}$$

When the concentration of nutrients becomes lower, the activity of cells becomes weaker. Therefore, we take that $a(A,N)$ is monotonically decreasing with N. On the other hand, the dependency of the active bacteria A on $a(A,N)$ can in principle be determined by their physiology, but is still unclear. In order to completely specify the form of $a(A,N)$, based on our observation the situation that if bacterial populations become quite sparse, each bacterium seems to be less active, we may assume that $a(A,N)$ is also monotonically decreasing with A. As an example of $a(A,N)$, we have the following form with switching mechanism:

$$a(A,N)=\begin{cases} a_0 & \text{for either } A<\theta_A \text{ or } N<\theta_N\,, \\ 0 & \text{elsewhere} \end{cases}$$

or, as a continuous function of $a(A,N)$, we may take

$$a(A,N)=\frac{a_0}{(1+A/\theta_A)(1+N/\theta_N)}\,,$$

where θ_A,θ_B and a are suitable positive constants.

Using suitable nondimensionless methods, we can rewrite (2.3) and (2.4) as the following RD system for the population densities of active and inactive bacteria u, w and the concentration of nutrients v:

$$u_t = \nabla(d(b)\nabla u) + uv - a(u,v)u\,,$$

$$v_t = \Delta v - uv, \quad t > 0,\ x \in \Omega\,,$$

$$w_t = a(u,v)u\,, \tag{2.5}$$

where with $b=u+w$, $d(b)$ is the ratio of the diffusion rates d_A and d_N. In our numerical computations, $a(u,v)$ is specified as

$$a(u,v) = \frac{1}{(1+u/a_1)(1+v/a_2)} \tag{2.6}$$

with suitable positive constants a_i $(i=1,2)$. This particular form is not essential to our result, and other forms also works well, if they are monotonically decreasing with u and v. We consider (2.5) in a two-dimensional bounded region Ω. The initial conditions are

$$u(0,x) = u_0(x) \geqslant 0\,,$$

$$v(0,x) = v_0 > 0, \quad t > 0,\ x \in \Omega\,,$$

$$w(0,x) \equiv 0\,. \tag{2.7}$$

From experimental requirement, we take $u_0(x)$ to be a delta-like function in the center of Ω and v_0 to be a positive constant in Ω. The boundary conditions on the boundary $\partial\Omega$ are

$$\frac{\partial u}{\partial n} = 0 = \frac{\partial v}{\partial n}, \quad t > 0,\ x \in \partial\Omega\,, \tag{2.8}$$

where n is the outward normal vector on $\partial\Omega$. It is noted that $d(b)$ and v_0 correspond respectively to the experimental parameters C_a^{-1} and C_n in Fig. 1.1. In fact, since an agar medium is mainly composed of water, the diffusivity of nutrient molecules d_N is not influenced very much by the variation of the agar concentration C_a. On the other hand, the motility of bacterial cells d_A depends strongly on C_a, resulting in the monotonic dependence of $d = d_A/d_N$ on C_a^{-1}.

If $d(b) = d$ and $a(u,v) = a$ are simply positive constants, the first two equations of (2.5) are exactly the same as the diffusive epidemic model [20]

$$u_t = d\Delta u + uv - au\,,$$

$$v_t = \Delta v - uv\,, \tag{2.9}$$

which is well known in mathematical epidemiology. Here u and v indicate, respectively, the infective and the susceptible species. It is shown in Hosono [21] that for any fixed d, if $a < v_0$, there are one-dimensional travelling wave solutions $(u(z), v(z))(z = x - ct)$ with velocity $c \geqslant 2\sqrt{d(v_0 - a)}$, while there is no such solution if $v_0 \leqslant a$. Furthermore,

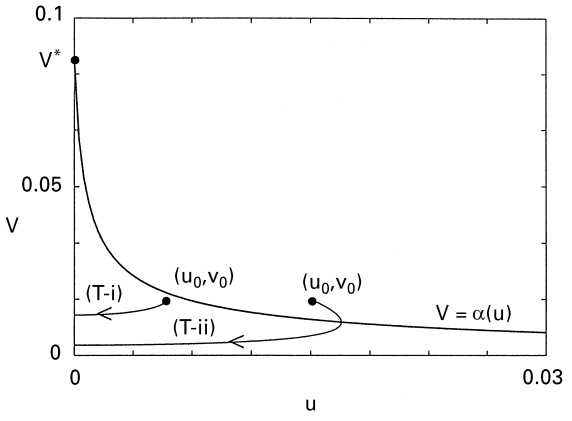

Fig. 2.1. Trajectories of solutions $(u(t), v(t))$ of (2.10).

it is numerically confirmed that these results are inherited from the two-dimensional situation, that is, under the initial condition (2.7), growth patterns are classified into two types only, even if d and v_0 are globally varied, that is, $u(t,x)$ either spreads as a ring-like pattern or fades out. This indicates that (2.9) generates neither any branching patterns nor concentric ring-patterns shown in Fig. 1.1.

Now, return to system (2.5). We first study its diffusionless system

$$\begin{aligned} u_t &= uv - a(u,v)u\,, \\ &\qquad t > 0\,, \\ v_t &= -uv\,, \end{aligned} \tag{2.10}$$

with the initial conditions

$$(u(0), v(0)) = (u_0, v_0) > 0\,. \tag{2.11}$$

It is obvious that $(0, \underline{v})$ is a critical point of (2.10) for any fixed $\underline{v} > 0$. The relation $a(u,v)=v$ leads to a monotonically decreasing function $v=\alpha(u)$ satisfying $\alpha(0)=v^* > 0$. One thus finds that $(0, \underline{v})$ is stable for any fixed $\underline{v} \in (0, v^*)$ and it is unstable for $\underline{v} \in (v^*, \infty)$. The transient behavior of $(u(t), v(t))$ of (2.10) and (2.11) is classified into the following two cases in the (u,v)-phase plane, as in Fig. 2.1:

(T-i) If (u_0, v_0) satisfies the inequality $v_0 > \alpha(u_0)$, the solution $v(t)$ is always monotonically decreasing with time t, while $u(t)$ first increases and then decreases, after crossing the curve $v = \alpha(u)$ vertically.

(T-ii) If (u_0, v_0) satisfies $v_0 < \alpha(u_0)$, $u(t)$ and $v(t)$ are both monotonically decreasing with t.

We note the situation where v_0 is close but below v^*. The solution $u(t)$ possesses excitable property, that is, if u_0 is small to satisfy $v_0 < \alpha(u_0)$, $u(t)$ monotonically decreases, while if u_0 is slightly larger to satisfy $v_0 > \alpha(u_0)$, it first increases and then decreases.

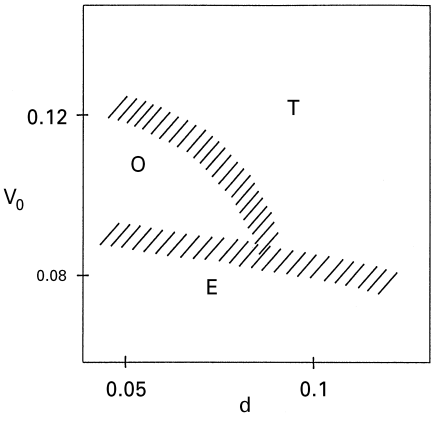

Fig. 3.1. Morphological diagram of (3.1) in the (d, v_0)-plane where $a_1 = \frac{1}{2400}, a_2 = \frac{1}{120}$, (T) travelling pulse of u, (O) oscillatory propagating pulse, (E) extinction of pulse.

3. One-dimensional growth patterns

In this section, we consider the one-dimensional problem of (2.5)–(2.7) in the semi-infinite interval $\mathrm{R}_+ = (0, +\infty)$. First, suppose the soft agar situation so as to assume that $d(b) = d$ is a constant. The resulting problem of (2.5) is simply written as

$$\begin{aligned} &u_t = d u_{xx} + uv - a(u, v)u, \\ &\qquad t > 0,\ x \in \mathrm{R}_+ , \\ &v_t = v_{xx} - uv \end{aligned} \tag{3.1}$$

with the boundary and initial conditions

$$(u_x, v_x)(t, 0) = (0, 0), \quad t > 0 \tag{3.2}$$

and

$$(u, v, w)(0, x) = (u_0(x), v_0, 0), \quad x \in \mathrm{R}_+ , \tag{3.3}$$

where $u_0(x)$ is a small droplet distribution at the end $x = 0$ and v_0 is constant. It is numerically shown that the asymptotic states of nonnegative solutions $(u, v)(t, x)$ of (3.1)–(3.3) are qualitatively classified into three cases, which are labeled by T, O and E in the (d, v_0)-plane, as in Fig. 3.1.

(A-i) In the region T, (u, v, w) takes the form of a propagating wave with constant shape and velocity [Fig. 3.2(a)].

(A-ii) In the region O, (u, v, w) takes the form of a propagating wave which oscillates in time and space [Figs. 3.2(b) and 3.2(c)].

(A-iii) In the region E, u gradually decays to zero and $u + w$ forms a stationary cluster [Fig. 3.2(d)].

The case (A-i) indicates the existence of travelling wave solutions $(u, v)(z)$ $(z = x - ct)$ with some velocity $c > 0$. This implies that the bacteria grow uniformly. On the contrary, (A-iii) means that the bacteria cannot continuously grow and eventually

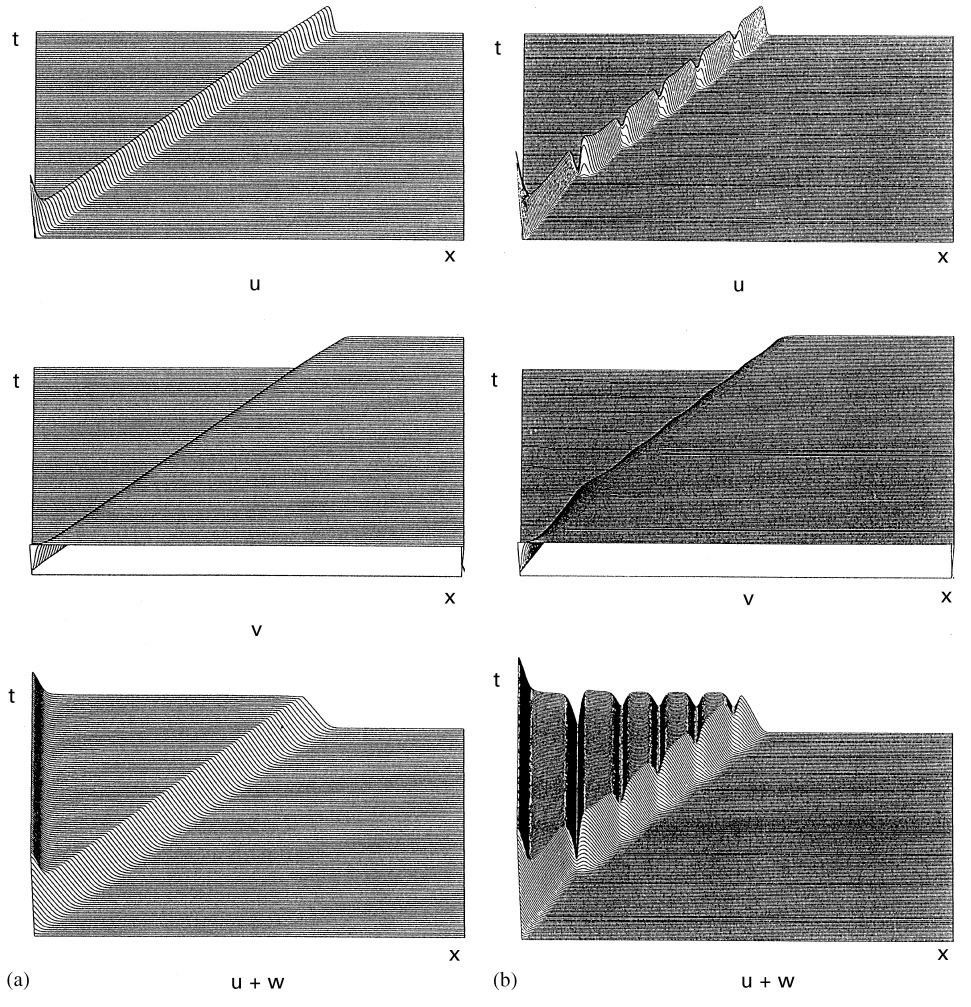

Fig. 3.2. Spatio-temporal profiles of u and $u+w$ where a_0, a_1, and a_2 are the same as the ones in Fig. 3.1. (a) Travelling waves ($d = 0.1$, $v_0 = 0.117$). (b) Oscillatory propagating waves ($d = 0.05$, $v_0 = 0.129$). (c) Oscillatory propagating waves ($d = 0.05$, $v_0 = 0.108$). (d) Clustering ($d = 0.1$, $v_0 = 0.0875$).

stop, because of poor nutrients. Let us explain the case (A-ii). Fix d and v_0 suitably to require the case (A-i). If d decreases with fixed v_0, the active bacteria u which propagate with constant velocity starts to oscillate with time, and the corresponding total bacteria b exhibit a static wave train with small amplitude [Fig. 3.2(b)]. When d decreases further, the oscillation becomes violent [Fig. 3.2(c)]. One thus expects that such an oscillatory propagating pulse appears as the consequence of Hopf-bifurcation of travelling waves arising in (A-i). We should remark that oscillating property of propagating pulses is quite similar to that of oscillatory propagation of flame front in the combustion equation when the Lewis number is smaller than unity [22].

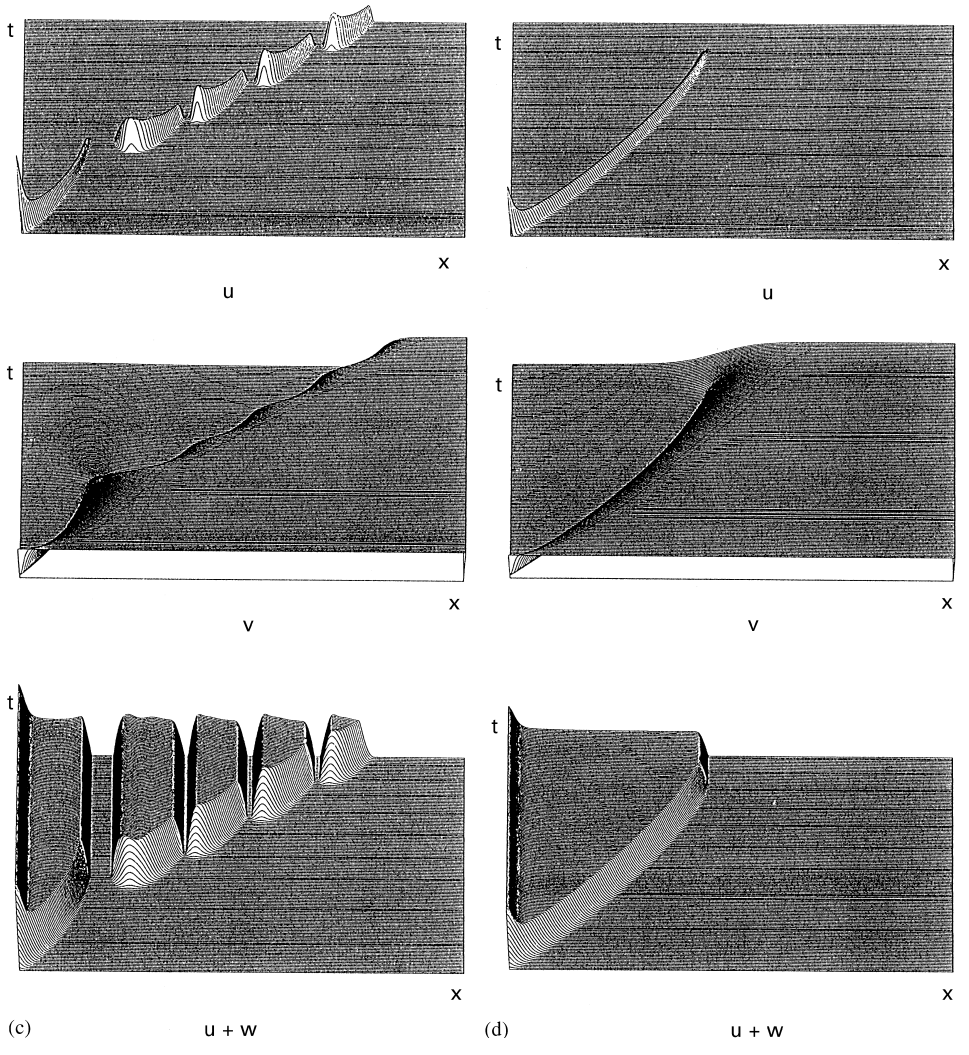

Fig. 3.2. Continued.

We next consider the hard agar situation and study the following nonlinear diffusion system in R_+:

$$u_t = d(bu_x)_x + uv - a(u,v)u,$$

$$t > 0,\ x \in R_+,$$

$$v_t = v_{xx} - uv, \tag{3.4}$$

where d is a positive constant. Here the boundary and initial conditions are the same as (3.2) and (3.3), respectively. A difference from the normal diffusion case is that (3.4) does not generate any oscillatory propagating pattern so that the asymptotic state

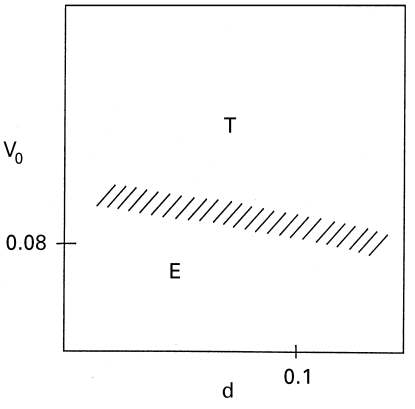

Fig. 3.3. Morphological diagram of (3.4) in the (d, v_0)-plane where $a_1 = \frac{1}{2400}$, $a_2 = \frac{1}{120}$.

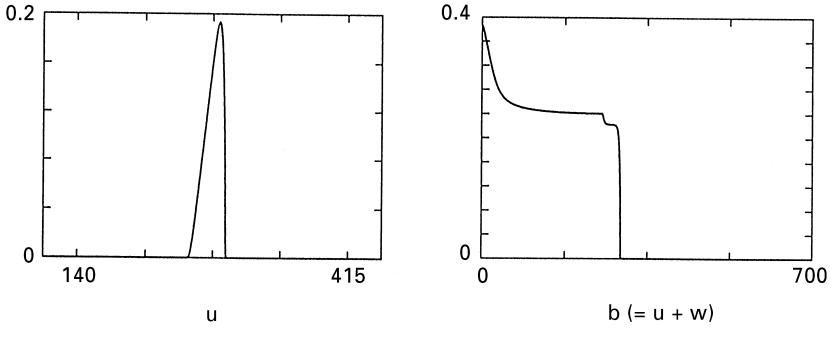

Fig. 3.4. The profiles of (u, v, b) in the region T where a_1, and a_2 are the same as in Fig. 3.1, $d = 0.05$ and $v_0 = 0.25$.

of solutions is classified into two types only, corresponding to (A-i) and (A-iii), which are respectively labeled by T and E, as in Fig. 3.3. The profiles of the solution (u, v, w) in the region T are almost similar to the ones in the normal diffusion case (Fig. 3.4) except for the appearance of interfaces in the fronts of u and b, because the nonlinear diffusion rate is degenerate where $b = 0$.

4. Two-dimensional growth patterns

We consider problem (2.5), (2.7) in a disk domain $\Omega = \{(x, y) \in \mathrm{R}^2 \,|\, x^2 + y^2 \leqslant r^2\}$ with suitably large radius r under zero-flux conditions on the boundary $\partial\Omega$, assuming that the initial distribution $u_0(x, y)$ as a droplet at the origin $(x, y) = (0, 0)$. We take d

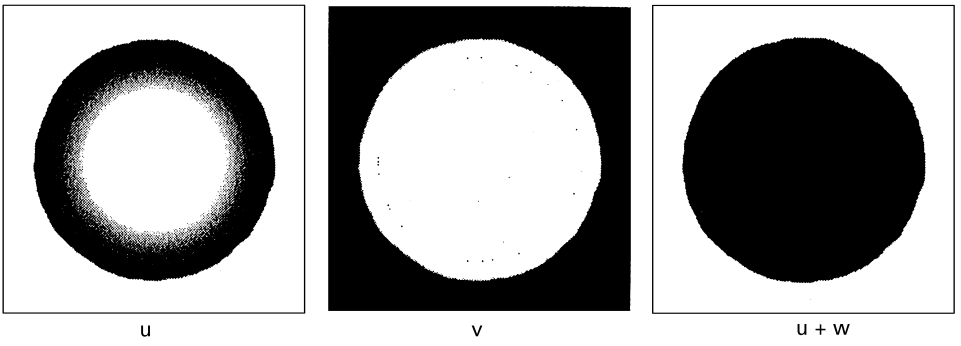

Fig. 4.1. A disk-like pattern of (4.1) where $d = 0.25$, $v_0 = 0.25$.

and v_0 as free parameters. By the one-dimensional results (A-i)–(A-iii) obtained in the previous section, one could easily expect the existence of radially symmetric patterns of the total bacteria $b = u + w$ exhibiting

(T-i) an expanding disk-like pattern;

(T-ii) an expanding concentric ring pattern;

(T-iii) a static small clustering pattern.

Keeping these radially symmetric patterns in mind, we numerically solve (2.5) and (2.7) in Ω, by using a finite element method with Delaunay triangulations [23].

4.1. Normal diffusion

We first consider the normal diffusion case where $d(b) = d$ for a positive constant d. The resulting system is

$$u_t = d\Delta u + uv - a(u,v)u\,,$$

$$v_t = \Delta v - uv, \quad t > 0,\ x \in \Omega\,,$$

$$w_t = a(u,v)u\,, \tag{4.1}$$

In computations, we always fix $a_1 = \frac{1}{2400}$ and $a_2 = \frac{1}{120}$. For v_0 and d large (nutrient-rich and soft environment), we find that (T-i) occurs, that is, u and b exhibit an expanding ring and disk-like patterns, respectively (Fig. 4.1). The latter pattern resembles the one in the region D in Fig. 1.1. When v_0 decreases, keeping d not so small, the ring pattern of u breaks down and splits into many spots which locate circularly, and each one spot splits into two, as if the process were self-replicating. When v_0 decreases further, tip-splitting of branches occurs frequently, and there appear DBM-like patterns which resemble the one in the region E (Fig. 4.2). Here we should note that such spot-splitting of u corresponds to tip-splitting of branches of b, which quite resemble the one in experiments [8] [Fig. 4.3(a) and (b)].

When d decreases, keeping v_0 small, the circular envelope of the DBM pattern is destabilized. Let both d and v_0 be small (but not sufficiently small) to require (A-iii),

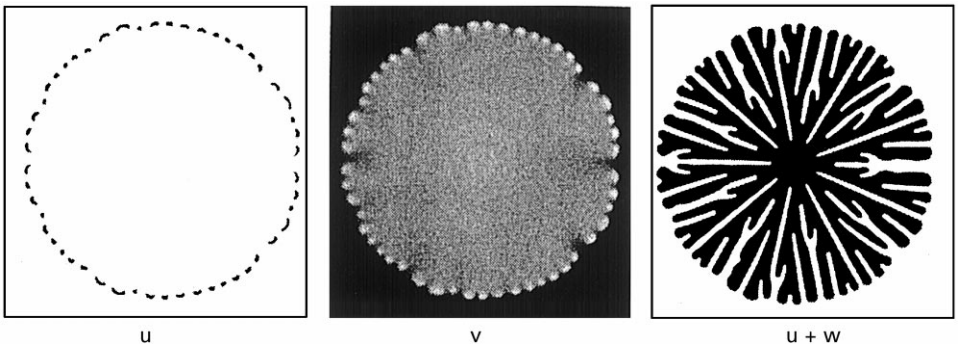

Fig. 4.2. A DBM-like pattern of (4.1) where $d = 0.12$, $v_0 = 0.071$.

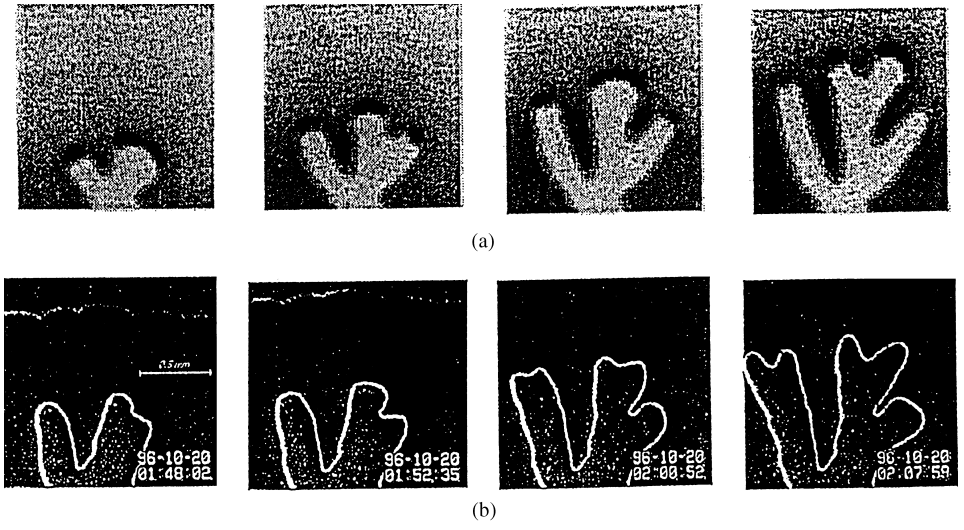

Fig. 4.3. Tip-splitting behavior in dendritic pattern: (a) numerical simulations of (4.1) (darker and brighter regions indicate active and inactive bacterial regions, respectively); (b) experiment.

that is, the situation where one-dimensional travelling pulses *never* exist. It is surprising that there appear two-dimensional spots of u which propagate very slowly outward, splitting into several spots many times. After long time, tiny spot patterns appear so that the total density b exhibit a DLA-like pattern which quite resembles the one in the region A (Fig. 4.4).

We next consider concentric ring patterns observed in the region C (Fig. 4.5). The process of growth is totally different from the above ones. They can be explained as follows: It essentially consists of two phases; growth and consolidation phases. In the growth phase, expanding branches which are populated by active bacteria with low density suddenly appear, keep expanding for a while, and then suddenly stop. In the consolidation phase, bacteria cannot move actively but they continue cell division so

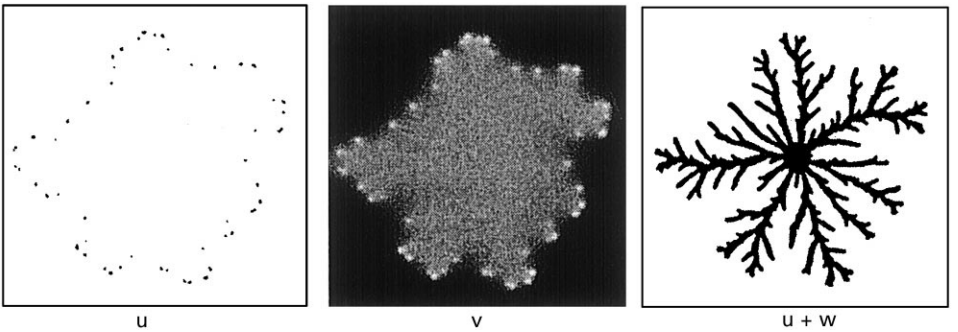

Fig. 4.4. A DLA-like pattern of (4.1) where $d = 0.05$, $v_0 = 0.087$.

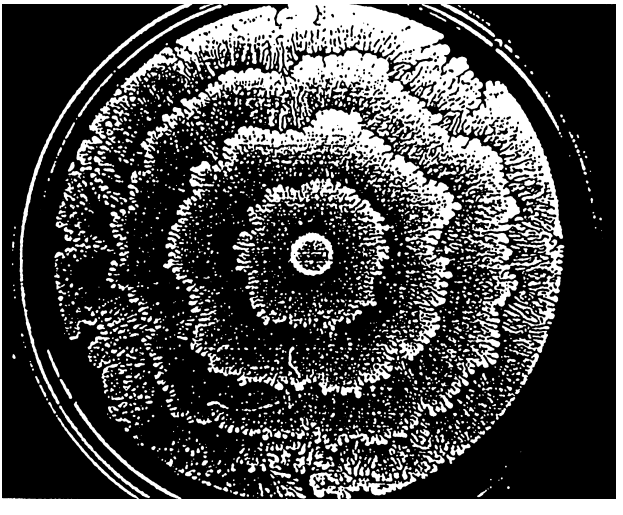

Fig. 4.5. A concentric ring pattern of bacteria in experiment.

that their density increases. In a few hours, bacteria pushing back and forth appear inside the colony. When this precursor activity reaches the interface of the colony, the branches suddenly start to expand again. Consequently, the concentric rings exhibit macroscopically a circular band. We next consider numerical concentric ring patterns generated by our model. By the case (A-ii), we expect the occurrence of concentric ring patterns. Indeed, (4.1) exhibits a concentric ring pattern, as in Fig. 4.6 where each ring exhibits branched structures. Two patterns observed in Figs. 4.5 and 4.6 seem to resemble each other.

Though more investigation is needed in modelling of periodic growth in the region C, our model may give a hint on the possibility of periodic growth of bacteria. Integarating the above ones, we can draw the morphological diagram of numerical colony patterns of (2.5) and (2.7) in Fig. 4.7.

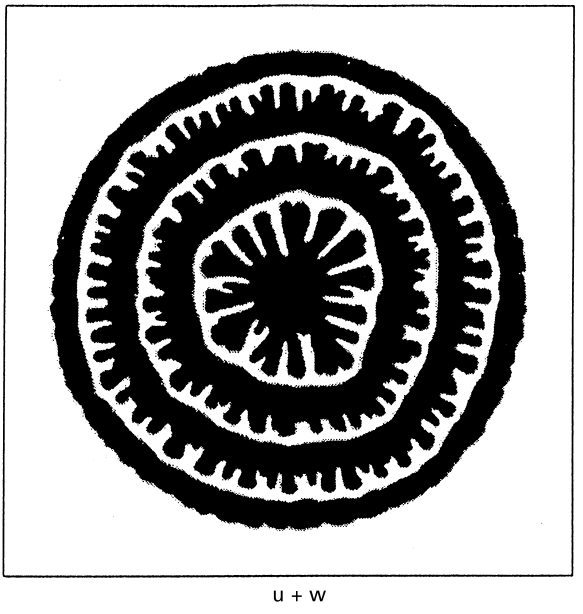

Fig. 4.6. A concentric ring pattern of (4.1) where $d = 0.05$, $v_0 = 0.1$.

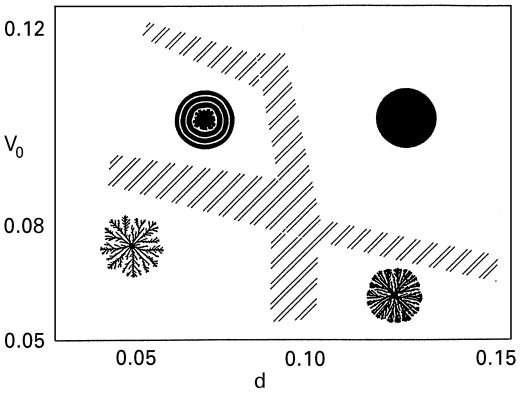

Fig. 4.7. Numerical phase diagram of colony patterns in the (d, v_0)-plane.

Finally, we remark on dense disk-like patterns with rough envelope in the region B. Model (1.5) with normal diffusion no more generates this kind of pattern. Since the situation indicates that the agar is hard, we replace the normal diffusion by the nonlinear diffusion in (2.5).

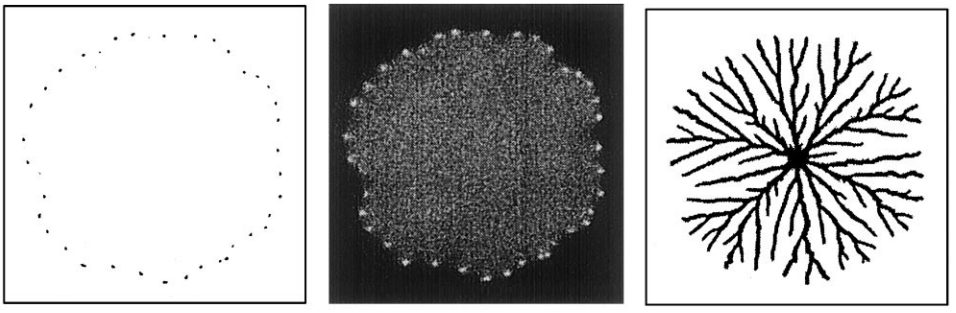

Fig. 4.8. A DLA-like pattern of (4.2) where a_1, and a_2 are the same as in Fig. 3.4, except $d = 0.05$ and $v_0 = 0.088$.

4.2. Nonlinear diffusion

In this section, instead of (4.1), we consider

$$u_t = d\nabla(b\nabla u) + uv - a(u,v)u\,,$$

$$v_t = \Delta v - uv, \quad t > 0,\ x \in \Omega\,,$$

$$w_t = a(u,v)u\,. \tag{4.2}$$

With d fixed small, we take v_0 as a free parameter. When v_0 is small (but not sufficiently small), (4.2) with (2.7) and (2.8) reproduce a DLA-like pattern in the region A, as in Fig. 4.8. This pattern is qualitatively similar to the one in Fig. 4.4. For the occurrence of DLA-like patterns, we emphasize that a suitable non-constant conversion rate is essential rather than the choice of either normal diffusion or nonlinear diffusion in our model. When v_0 increases, each branch in the DLA-like pattern becomes thicker and thicker and finally there appears a dense disk-like pattern with rough envelope in the region B, as in Fig. 4.9(a). This morphology is quite reminiscent of the experimental one, as in Fig. 4.9(b) [1].

5. Concluding remarks

We have proposed a phenomenological RD system model to describe the growth patterns of bacteria. In spite of the fact that the system looks so simple, it generates surprisingly rich patterns, depending on values of d and v_0. A feature of our model is that the state dependent conversion rate from the active cells to the inactive ones is included, which is essentially different from any other already proposed RD models such as Kitsunezaki's model (1.9). We emphasize that our model generates four different types of patterns, except for compact patterns with rough interface observed in Region B, only by changing two parameters d and v_0, which correspond to the concentrations of

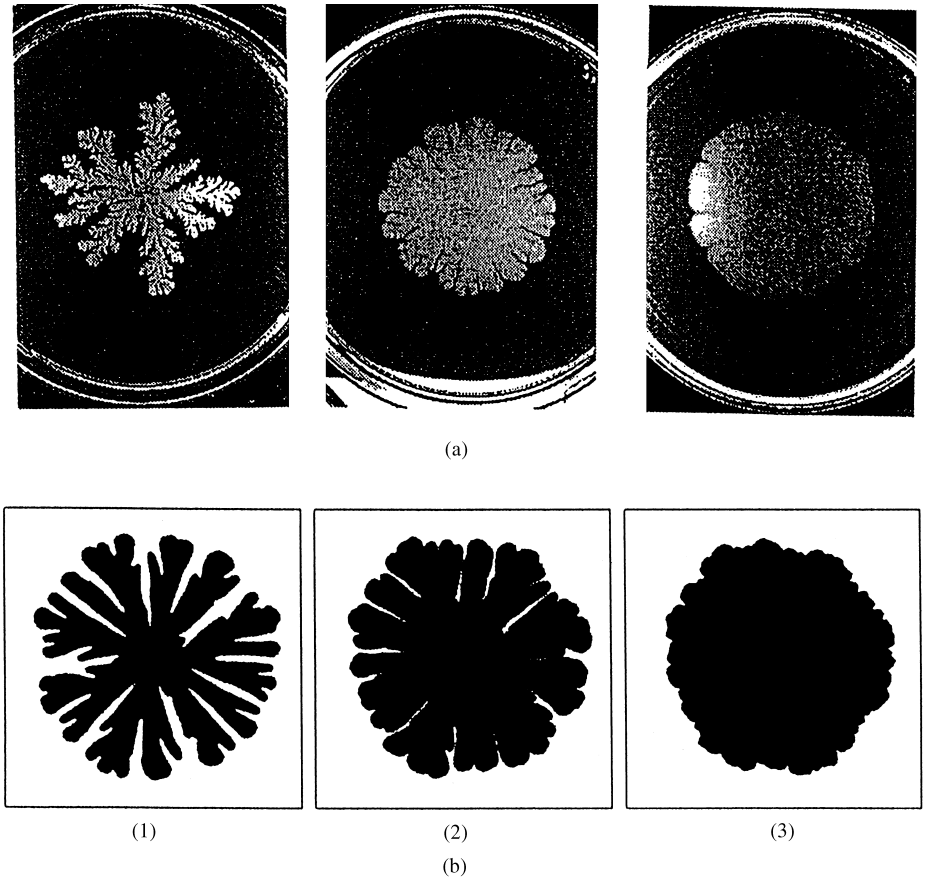

Fig. 4.9. Morphological crossover from DLA-like (region A) to dense disk-like pattern with rough envelope (region B): (a) experiment; (b) numerical simulation of (4.2) ((1) d=0.05, v_0=0.125, (2) d=0.05, v_0=0.167, (3) $d = 0.05$, $v_0 = 0.25$).

agar and nutrient. As for the compact patterns with rough interface, one can reproduce them by taking nonlinear diffusion into account.

Acknowledgements

The authors would like to thank Mr. Shintaro Takeuchi for helping with numerical simulations of the model in Section 4.

References

[1] M. Ohgiwari, M. Matsushita, T. Matsuyama, J. Phys. Soc. Japan 61 (1992) 816.
[2] M. Matsushita, in: J.A. Shapiro, M. Dworkin (Eds.), Bacteria as Multicellular Organisms, Oxford University Press, New York, 1997, pp. 363–393.

[3] J. Wakita, K. Komatsu, A. Nakahara, T. Matsuyama, M. Matsushita, J. Phys. Soc. Japan 63 (1994) 1205.
[4] M. Matsushita, H. Fujikawa, Physica A 168 (1990) 498.
[5] T.A. Witten, L.M. Sander, Phys. Rev. Lett. 47 (1981) 1400.
[6] F. Family, T. Vicsek (Eds.), Dynamics of Fractal Surfaces, World Scientific, Singapore, 1991.
[7] J. Wakita, H. Itoh, T. Matsuyama, M. Matsushita, J. Phys. Soc. Japan 66 (1997) 67.
[8] J. Wakita, I. Ráfols, H. Itoh, T. Matsuyama, M. Matsushita, J. Phys. Soc. Japan 67 (1998) 3630.
[9] I. Golding, Y. Kozlovsky, I. Cohen, E. Ben-Jacob, Physica A 260 (1998) 510.
[10] E. Ben-Jacob, O. Shochet, A. Tenebaum, I. Cohen, A. Czirók, T. Vicsek, Nature 368 (1994) 46.
[11] K. Kawasaki, A. Mochizuki, M. Matsushita, T. Umeda, N. Shigesada, J. Theor. Biol. 188 (1997) 177.
[12] S. Kitsunezaki, J. Phys. Soc. Japan 66 (1997) 1544.
[13] Y. Kozlovsky et al., Phys. Rev. E 59 (1999) 7025.
[14] A.M. Lacasta et al., Phys. Rev. E 59 (1999) 7036.
[15] J. Monad, Recherches sur la croissance des cultures bactériemes, Hermann, Paris, 1942.
[16] D.A. Kessler, H. Levine, Nature 394 (1998) 556.
[17] M. Mimura, H. Sakaguchi, M. Matsushita, Kyoto Conference on Mathematical Biology, 1996.
[18] T. Matsuyama, M. Matsushita, in: P.M. Iannaccone, M. Khokha (Eds.), Fractal Geometry in Biological Systems, CRC Press, Boca Raton, FL, 1996, pp. 127–171.
[19] A. Okubo, Diffusion and Ecological Problems: Mathematical Models, Springer, Berlin, 1980.
[20] W.O. Kermack, A.G. McKendric, Proc. R. Soc. A 15 (1927) 700.
[21] Y. Hosono, B. Ilyas, Math. Models Methods Appl. Sci. 5 (1995) 935.
[22] P.C. Fife, Regional Conference Series in Applied Mathematics, Vol. 53, SIAM, Philadelphia, PA, 1988.
[23] D.F. Watson, Comput. J. 24 (1981) 167.